Vol. 1, No. 3 (2025)

Open Plasma Science

Regular article

History

Received November 14, 2024

Revised February 18, 2025

Accepted March 13, 2025

Published April 8, 2025

Identifiers

DOI 10.46298/ops.14788

HAL -

ArXiv -

Zenodo 14178090

Supplementary Material

-

Update of the integrated flight simulator for ASDEX Upgrade

Pierre David[*,1], Emiliano Fable[1], Chuanren Wu[2], Matthias Gehring[1], Michael Sieben[1], Berhnard Sieglin[1], Giovanni Tardini[1], Wolfgang Treutterer[1], and the ASDEX Upgrade team[a]

[1]Max Planck Institute for Plasma Physics, Boltzmannstr. 2, 85748 Garching, Germany

[2]Karlsruhe Institute of Technology, Institute for Pulsed Power and Microwave Technology, Hermann-von-Helmholtz-Platz 1, 76344 Eggenstein-Leopoldshafen, Germany

[a]see the Author list of H. Zohm *et al.*, 2024 *Nucl. Fusion* 64 112001, doi: 10.1088/1741-4326/ad249d

Abstract

We present the latest updates of the flight simulator of ASDEX Upgrade (AUG), 'Fenix AUG'. Fenix AUG contains simplified models for both the plasma physics and the device operation. The updated version is split into three independent repositories and has been integrated into Docker containers for better management and deployment. The device models can now directly import their configuration from the AUG control system. Although the physics models can be fine tuned to each case, the default settings have been set up to run a large variety of experiments without the need of case-to-case adaptation. Together, the enhancements make Fenix AUG a versatile tool that can be applied to a wide range of applications 'out-of-the-box', such as: to compare simple physics models to the experiment, to assess new controllers within the framework of the existing ones, or, to verify that a planned discharge will follow expected trajectories and will not run into machine or safety limits. An example of each application is showcased to highlight some strengths and limitations of the simulator.

Keywords— Flight simulator, Plasma control, Simulation

* Corresponding author: pierre.david@ipp.mpg.de

Cite as: David *et al.*, Update of the integrated flight simulator for ASDEX Upgrade, *Open Plasma Science* 1, 3 (2025), doi: 10.46298/ops.14788

Contents

1 Introduction

Future fusion devices are complex systems and present day experimental devices need an additional versatility to test as large a parameter set as possible. To that end, more and more advanced control and monitoring strategies, and (virtual) actuators are used [MP19, YGY+21, NMS+23, BvG+23, dCD+24], such that although each element is still well known in control theory, the system's behavior exceeds the predictability of its individual components. As a result, being able to run simple yet realistic enough simulations that include the plant systems, the plasma and their interactions became particularly important. Such a simulation platform shall here be called *flight simulator*, and has the experimental discharge program as input, and time evolution of both the plant and the plasma quantities as outputs. The current paper reports on major upgrades of the flight simulator called *Fenix*, previously introduced in [JFET21] and [FJT+22]. Fenix has three main components: one machine independent, called Fenix Core [WDF+24], one machine dependent for the machine systems 'Fenix Device' also serving as Graphical User Interface (GUI) for the flight simulator, and one that regroups all physics models, ASTRA 8 and its modules [TFA+24]. This architecture is depicted in Figure 1. Fenix device is a Simulink® model using MATLAB® versions R2022b [Mat22] or R2023a, up from R2019b previously used. The use of versions newer than R2022b was particularly motivated by its native support of VNC (Virtual Network Computing) and web browser mode, a major convenience for the use of Docker [Mer14] and Apptainer (Singularity) [KcB+21] containers, as will be described later. However, more recent MATLAB® versions lose compatibility due to the use of deprecated MATLAB® functions in PCSSP (Plasma Control Systems Simulation Platform) [WAD+15]. An ongoing, independent, revision of PCSSP will alleviate version requirements.

The PCSSP library is used to manage MATLAB® and Simulink® simulation environment, as well as for its library blocks for the pulse supervisor, compact controllers and monitors. The development of PCSSP is

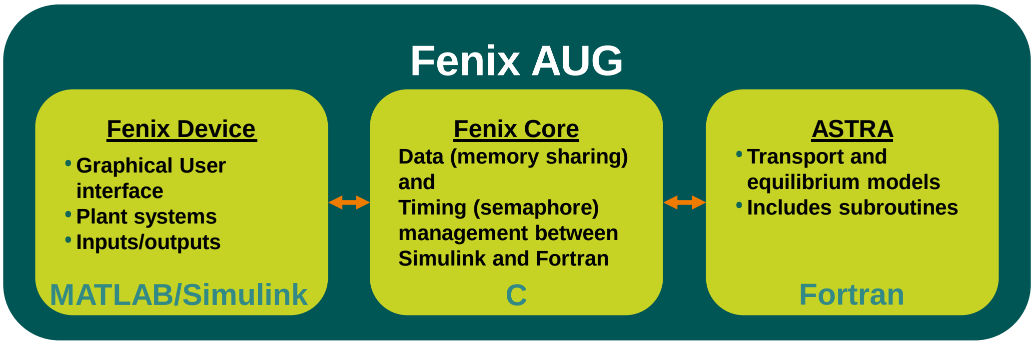

Figure 1: Structure of Fenix AUG, divided into Fenix Device, that includes the Graphical User Interface and the models for the plant systems, Fenix Core and ASTRA.

directed and funded by ITER Organization, and primarily aims at aiding the development and testing of ITER control systems. Using PCSSP for Fenix allows for mutual benefits between the ITER and Fenix teams: the application of Fenix to the ITER Discharge Control System is then straight forward, and Fenix gains from the flexibility, modularity and independent developments of PCSSP. The Fenix version detailed here is the one used for AUG, however other devices are being modeled and developed in Fenix as well: DEMO [dFF+23], ITER and TCV [CFS+24].

Fenix has been developed for three main use cases. The first one is a validation of a discharge program before an experiment. Once a discharge program has been developed, it can be run on Fenix to check that the combination of requested values, each within their individual boundaries, will not violate machine limits once combined, and that the discharge should go in the relevant parameter range for the proponent. The second use case is to utilize Fenix as a test bench for controllers development and improvement. The controllers can then be tested within the context of the intricate feedback loop of the plasma and the combination of all other controllers. Lastly, the third main use case, is to be able to more easily compare simple plasma models to experiments. By implementing the model to be validated in the modular ASTRA code, Fenix simulations can be directly compared to experiments using the same input (the discharge program).

In the following, the paper is divided in two major sections. Section 2 describes the current status of Fenix, focusing on Fenix Device. Then, examples of simulations are given in Section 3 to showcase some capacities and limitations of the software.

2 Fenix description

The Fenix AUG upgrades reported here are mostly twofold. First, the architecture of the code has been cleaned, allowing full version control using three independent repositories. Second, they aim at bringing the model for the machine systems closer to the ones of AUG [TCL+14, KDG+24]. In this section, we will introduce Fenix device, also serving as Graphical User Interface (GUI), in 2.1. Then, the main updates of Fenix AUG from the previous versions are described in 2.2, before focusing on the newly enabled code management in 2.3. Subsection 2.4 details the elements of the control system in the latest model. In the end, the computational times are discussed in 2.5.

2.1 Fenix device structure

The main GUI for Fenix AUG, shown in Figure 2, is the Simulink® model for Fenix device. It is visually separated into four groups: *discharge setup*, *Fenix configuration*, *Plant* and *control system*. The Simulink® masks for the blocks in the *Fenix configuration* area are GUIs where the user can interactively manage their

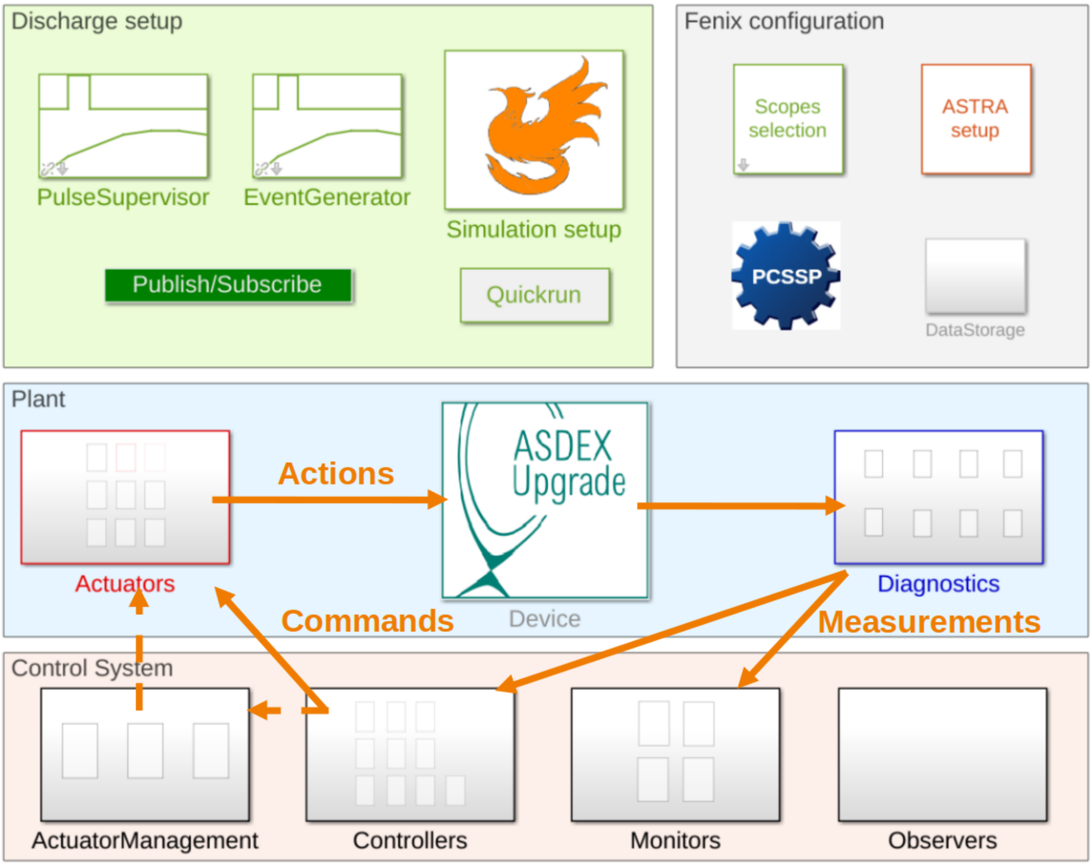

Figure 2: Fenix Device, the Simulink® model of Fenix AUG, also serving as Graphical User Interface. The orange arrows are added to highlight the typical signal route but are not part of the interface. The central block 'Device' contains the S-function connecting to Fenix Core and ASTRA.

folders setup, scope displays and the interface with the ASTRA code. Once Fenix is setup, there are few reasons to use the *Fenix configuration* corner again. The *discharge setup* blocks are to manage simulation inputs and to configure the model's subsystems. The discharge program is directly loaded from the same xml file used to run AUG. The rest of Fenix Device can be manually configured, but the most common approach is to use the scripts from the mask *Simulation setup* to setup Fenix as was AUG for a given discharge. These scripts configure the controllers and monitors using the xml files from the AUG control system, and the power supplies (described in subsection 2.4) from the same parameters as AUG. Therefore, Fenix simulations can directly be put side to side to their experimental equivalent. Finally, the block *Publish/Subscribe* is the PCSSP library used to connect the inputs and outputs of all subsystems. Due to the complexity and the required high flexibility of the Fenix Device model, using Simulink® busses to manage the communication between all the subsystems would clutter the interface and make the addition or edition of subsystems very tedious. The library was inspired by the same system from AUG discharge control system of AUG, detailed in [TCL+14]. In short, each element of the control system 'publishes' its list of output signals and lists the input signals it needs to 'subscribe' to. Then, the library checks the uniqueness of published signals and the availability of all required signals, before establishing all the connections.

Discharge programs of AUG are split into so-called *segments*, like for Wendelstein 7-X [SNL+06] and currently planed for ITER. Each segment has its own technical or physics goal, for instance, spinning up the flywheels, initiating plasma breakdown, managing the trajectories during plasma flattop or ramping down the plasma. There are also optional segments such as soft-emergency ramp-down, or immediate stop of the plasma [NER+07]. Each segment has a set maximum run time, called *watchdog time*, and can have conditional segment branching for exception handling. As a result, some segments can be re-used within a discharge or between different discharges. The segment logic is encapsulated in the Pulse Supervision Controller module of PCSSP, which finally outputs reference waveforms. Replacing this module or defining a single segment allows to use Fenix in an environment without segments. Since Fenix is not limited by physical or safety constraints to load the power supplies or ramp up the coils currents, the phases preceding the breakdown are usually shortened from a couple minutes, down to 1.6 seconds, to avoid meaningless simulation time.

2.2 Updates from previous Fenix versions

	Status in [JFET21] and [FJT+22]	Current manuscript and [FTGt25]	ETA for future updates
Demonstration on manually configured models of the machine	✓	✓[1]	
Version control	$\mathcal{P}$	✓	$\sim$ 1 year[2]
Interface between ASTRA and Simulink®	$\mathcal{P}$	✓ [WDF+24]	
Native use of PCSSP controllers and monitors, importing setup from AUG	$\mathcal{P}$	✓[3]	
Power supply connections and configuration identical to AUG		✓[4]	
Docker/Apptainer Containerization		✓	
Non-interactive version (*typ.* for batch runs)			$\sim$ 1 year
Continuous Integration and Quality Assurance		$\mathcal{P}$	$\sim$ 2 year[5]
Upper divertor coils and power supplies		✓	
Actuator management		$\mathcal{P}$	$\sim$ 1 year[6]
ICRH power deposition		$\mathcal{P}$	$\sim$ 2 years[7]

Table 1: Current status of Fenix compared to past publications and future plans. The letter $\mathcal{P}$ stands for 'partially implemented'. The annotations are detailed in the text of Section 2.2

The most significant upgrades of Fenix AUG since the last reports are summarized in Table 1. The annotations therein are developed here:

1 The former version of Fenix AUG showcased the feasibility of such a flight simulator. However, it could only be run by its main developers due to its complexity. A full manual configuration is still possible, although obsolete in most cases.

2 While Fenix Core, Fenix Device and ASTRA are now in independent repositories, the implementation of a meta-repository also managing the containerization is planned for the near future.

3 The configuration for the controllers and monitors is loaded from the xml files from AUG.

4 The power supplies configurations and their connection to the coils use the same parameters than AUG.

[5] Continuous Integration and Quality Assurance are under development. Given the complexity and the many layers of Fenix, defining and implementing a meaningful set of requirements will extend to several years.

[6] The actuator management of Fenix is a simplified model of each independent heating system of AUG. The real system from AUG [KTS+20] will be implemented, enabling the import of the exact rules from AUG and combining the different heating systems.

[7] The actuator and control loop for the ICRH systems are implemented according to DCS and the power deposition is modeled by a Gaussian. There are ongoing activities to simulate the ICRH power deposition using surrogate models, targeted at real-time applications.

2.3 Code management and integration

As already mentioned, one of the major technical upgrades of Fenix AUG is its separation into the three components Fenix Device, Fenix Core and ASTRA, each maintained in their own repository. Fenix Core and Fenix Device contain the machine-agnostic and machine-specific (respectively) flight simulator configuration files that need to be shared to ASTRA. As such, any version of ASTRA 8 can be used, regardless of the exact configuration or list of sub-modules and functions, and does not need to be adapted to the flight simulator. Typically, the newer developments including models such as TGLF-SAT2 or FACIT [AGT+22, FAD+24], or integrated modelling [LAD+20] can be used with Fenix, but are part of distinct work, as their long simulation times defeat the current purpose of a flight simulator. Similarly, STRAHL [Dux06] is disabled in Fenix simulations.

The second principal upgrade is the development of Docker and Apptainer images, encompassing all the prerequisites to operate, compile, and run Fenix AUG and was aimed at accomplishing two main objectives. The first objective is that it efficiently standardizes the necessities for compilers, libraries, and specific versions of MATLAB® and Simulink®. The use of GUI is enabled by connecting to the container via VNC or Web browser, either by the use of a virtual desktop inside the Docker container or by using the native MATLAB® option, for versions more recent than 2022b. The Apptainer solution also offers to forward the MATLAB® windows outside the container directly. The second objective is to set a suitable environment for utilizing Continuous Integration (CI) tools such as Jenkins, already used for many AUG codes. In the near future, a meta-repository will be created for Fenix AUG, in order to oversee the versions of each repository and include the use of CI down to the containerization. At the same time, a version of Fenix AUG without GUI is being developed ('headless' version), allowing for batch runs. In turn, this will support the definition and implementation of unit tests. Currently, instead of unit testing, Fenix AUG is assessed by configuring and running a simulation for discharge #40446, which will be presented in Section 3. However, there is currently no quantitative assessment of functionality. Similarly, the implications of the closed control loop will be investigated in a dedicated work. The now stable and reliable architecture and communication between Simulink® and ASTRA will allow for analyses of numerical approximations and discretization, and on the time steps variability of the Simulink® solver.

2.4 Controllers, actuators and diagnostics

In the lower two thirds of the interface in Figure 2, the signal communication is displayed with the orange arrows, omitting the requested trajectories (both feedforward and feedback) from the Pulse Supervisor to the controllers, and the monitored signals sent to the Pulse Supervisor for segment branching. The signals follow the same route as in the experimental setup: the controllers send the required commands to the *actuators*, that generate the input values for ASTRA, which replaces the plasma. In turn, the signals from ASTRA are transformed into the same format than the machine's diagnostics, and are finally sent to the controllers and monitors. The actuator management handles and assigns actuation resources. At AUG it is currently only used for heating, but the same method developed at ITER is also applied for fueling.

The controllers are separated into the same groups as for AUG, each using a 'compact controller' module from PCSSP [TZM+05, TRR+17]: plasma current, plasma position, plasma shape, gas fueling, pellet injection, plasma radiation, and heating systems (Neutral Beam Injection (NBI), Electron Cyclotron Resonance Heating (ECRH) and Ion Cyclotron Resonance Heating (ICRH)). To allow backward compatibility with older campaigns of AUG where the controllers were grouped differently, former setups are also present and the model can automatically switch configuration when needed.

The implemented monitors are the coils currents and forces monitors, also based on PCSSP modules, ensuring that the monitored values stay within set limits. In particular, monitors can trigger segment branching, either to try a recovery or to safely terminate the plasma. Tracking the monitors outputs is a main component to validate discharge programs (the first described application of Fenix), checking that they would not run into foreseeable limits.

The different actuators have their own simplified models. The three heating systems balance the requested heating power among their different channels according to their individual availability and priorities. The pellet launcher is modeled with a system that can both fire individual pellets from direct triggers in the discharge program and converts requested pellet frequencies into waiting time between pellets. Pellet sizes, delay and success rate are free parameters. The gas system simulates the connection of AUG with the different divertor and midplane valves being connected to up to five different gas channels. The two main AUG flywheels are modeled by connecting their rotating speed and stored energy through their moment of inertia. The magnetic coils' power supplies and heating systems then consume this energy. The three heating systems are scaled by an estimate of their efficiencies, and the power required by the coils is proportional to their integrated squared current $\int i^2 \mathrm{d}t$. The last actuators are the power supplies. They are subdivided the same way AUG system is, meaning they are divided into *units* [KGS+15] with different capabilities and configurable setups, and each coil can be connected to (almost) any unit. Once again, to allow backward compatibility, former units are still available and the configuration of all units can easily be swapped between old setups and the current one. As a note, the magnetic perturbation coils power supplies are not included here, as their setup is unique and their power load much smaller than the other ones, thus can be neglected, and, there is no physics model for the interaction of these coils on the plasma in Fenix.

Finally, the central block is where the communication with ASTRA is done by calling Fenix Core as a Simulink®'s *S-function*. Fenix Core uses shared memory and semaphores for the synchronisation and communication between Simulink® and ASTRA. Its flexibility allows to adapt to different devices and easily change the configuration of either ASTRA or Fenix Device.

2.5 Configuration and run times

Over the different phases, Fenix uses up to 4 cores and 20GB of virtual memory. The larger part of the memory is used during the compilation of the Simulink® model (Fenix Device). The following benchmark numbers are given when running Fenix container on a local machine with an Intel(R) Xeon(R) W-2245 CPU @ 3.90GHz and have a large variation due to the high diversity of setups. Configuring all of Fenix for a new simulation, (setting up the discharge program, controllers, monitors and power supplies), takes about 1 to 5 minutes. Given the required high flexibility of Fenix, the default, faster tools from Simulink® for controllers and signal generation cannot be used. Consequently, custom solutions have been developed within PCSSP. The long configuration time is due to PCSSP being based on the Simulink® block interface, meaning that a reconfiguration changes the Simulink® model iteself. An update is planned to switch as much of the configuration to MATLAB® functions and Simulink® dictionaries, limiting the dynamic blocks edition. Afterward, simulating a full 10 to 13 seconds of experiment (up to 10 seconds of plasma, plus the shortened coils and power supplies ramp up), takes about

5 to 10 minutes. In order to maximize user-friendliness despite its complexity, some inefficient actions are kept during runtime, such as plots and log file writing, requiring access to both the display and the file system. These could be deactivated to speed up the simulation time by about 20-30%, but as of yet, Fenix is designed for case-by-case simulation monitoring instead of, for instance, parameter scans.

3 Examples of run

In this section, five examples of runs will be shown: a so called AUG 'standard H-mode' (subsection 3.1), the introduction of a reduced model for core impurities content (subsection 3.2), an estimation for an upcoming controller of the power crossing the separatrix (P_{sep}) (subsection 3.3), the validation of the models during vertical displacement events (VDE) experiments (subsection 3.4), and estimations of experiments with the new upper divertor of AUG (subsection 3.5). The different scenarios all use the same configuration for the ASTRA models and no tuning has been made to better fit the experimental time traces. The goal here is to display the capabilities of the standard setup of Fenix when importing the control system configuration from AUG. As a result, the physic results are not discussed in details, as each example would be the topic of its own dedicated work.

3.1 Standard H-mode (#40446)

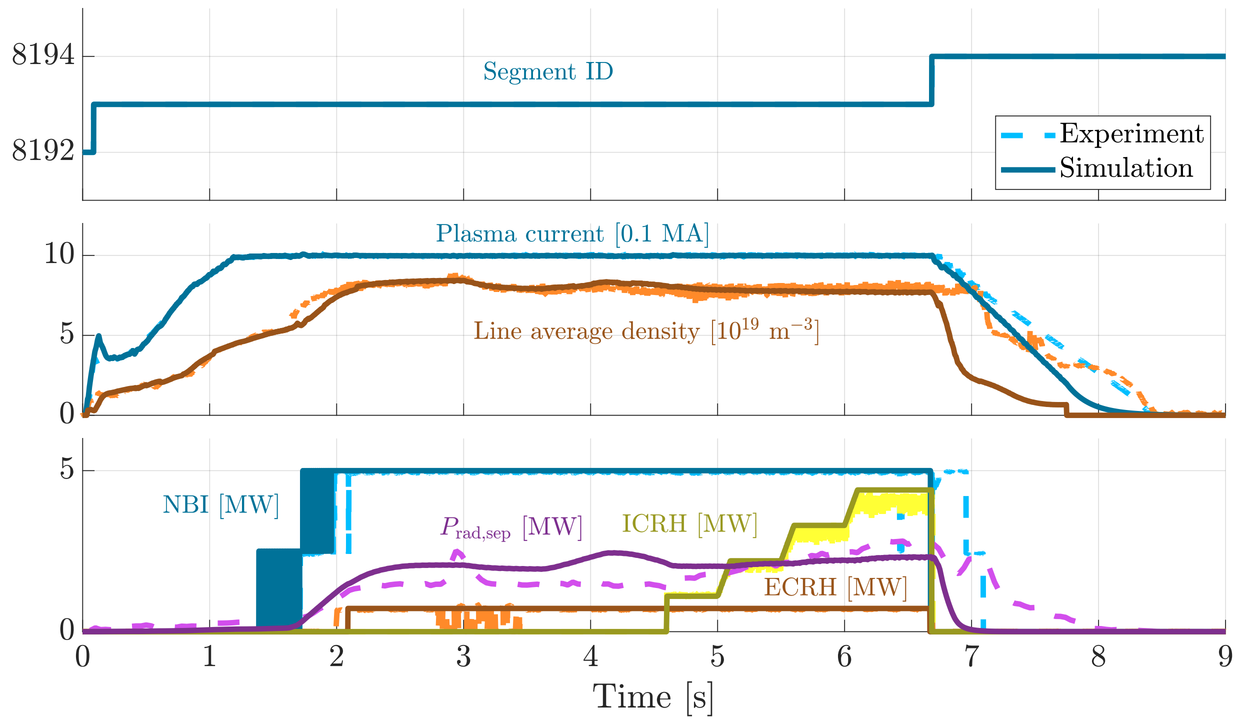

Figure 3: Segments branching (top) Plasma current and line averaged density (middle) and power balance (bottom) for the standard H-mode discharge #40446 (dashed lines, lighter colours) and Fenix simulation (full lines, darker colours) with the same configuration and discharge program.

'Standard H-mode' at AUG are high confinement regimes, or H-mode, with nominal values for all systems, used to check that the different systems and diagnostics are working as expected. Consequently they use most systems, but none with extreme values, and are a good test case for Fenix. Figure 3 displays the time traces for the segment branching, the plasma current and integrated density and the input and radiated power for one of the latest standard H-mode run on AUG. In all cases, the experimental values are plotted for #40446 (in dashed lines) along with the simulation ones (in full lines), both using the exact same discharge program and configurations.

For the plasma ramp up and flat top, the time traces for the plasma current directly overlap, and the simulated density is almost always within the experimental fast variation. The larger discrepancy shortly before two seconds is likely linked to the L to H transition, modeled by a change of pedestal when the input power crosses the L-H threshold scaling [MTtI08], being too simplistic. Since this discharge is one of the references used to validate the accuracy of Fenix, the different free parameters are also best tuned for it. The top plot, showing the evolution of the discharge segment, showcases that the segments branching happen at the same time, in this case they all reached their watchdog time. The radiated power, shown in the lower plot, is underestimated, especially in sections with very low radiation. The radiation peak happening in the experiment shortly before three seconds is a sudden tungsten flux. This outlier is planned to be explored in the future, using the event generator of Fenix. The ECRH power oscillation happening around that time (2.8 to 3.3 s) is an internal test from the heating system (not included in the discharge program), alternating between each of the eight gyrotrons twice, and is independent from the radiation event. Another potential shortcoming is the particle balance, that only has a particularly reduced model, as edge transport challenges even SOLPS-ITER modelling performed for AUG [WSW+21], so a one dimensional fast code can only be very approximate. In ASTRA, the particle source inside the separatrix is taken as a proportional value of the gas valves opening and their position, based on experimental results and more advanced models. This allows for a reasonable reconstruction of the density profile in most common cases, but the particle balance in the scrape-off-layer is only an estimation.

The ramp-down phase is where the time traces deviate the most from the experiment. Indeed, there has until very recently not yet been any focus on optimizing the models for ramping down the plasma, and is therefore known to be the least precise transient model. Recent investigations into the ramp-down evolution in Fenix have revealed three potential candidates that could improve the accuracy of the simulations for the plasma termination, if properly addressed together. First, the modeled pedestal stability, which assumes a peeling-ballooning limited pressure gradient, deviates from the experimental one during the current decrease. Including a critical pressure limit scaling with the plasma current (such as the one presented in [LAD+20], for instance), could improves the pedestal pressure evolution. Secondly, the lack of model for the scrape-off-layer and divertor region results in a much too strong density decrease when cutting the gas fueling, especially at lower currents. Finally, ramping down from H-mode necessarily includes the H-L back transition, which then happens at low density and current, where the known scalings become less accurate. However, further research is still required to develop robust and generic enough models, especially for the last two points.

3.2 Impurity model (#40250)

As discussed in the previous example, simplified models for radiation and impurities transport still have difficulties reproducing even simple experimental conditions. Recently, a new model for the divertor enrichment of impurities in AUG has been published [KDH+24]. The model only uses engineering parameters to estimate the impurity concentration at the outer core, making it usable as time dependent boundary conditions for simulations in Fenix AUG. It has been implemented in Fenix for neon, argon and krypton. A test case discharge of AUG is #40250 (also used in [KDH+24]), where argon is used as an actuator for detachment control from 3 to 4.2 seconds and is then frozen to its last value, and two decreasing ramps of nitrogen are performed one after the other. For the simulations, since there is no detachment model to control the argon gas valves, the experimental values have been used as feedforward ones. Figure 4 showcases the time traces from the simulation and its experimental counterpart (#40250) for the density, the power balance and the gas

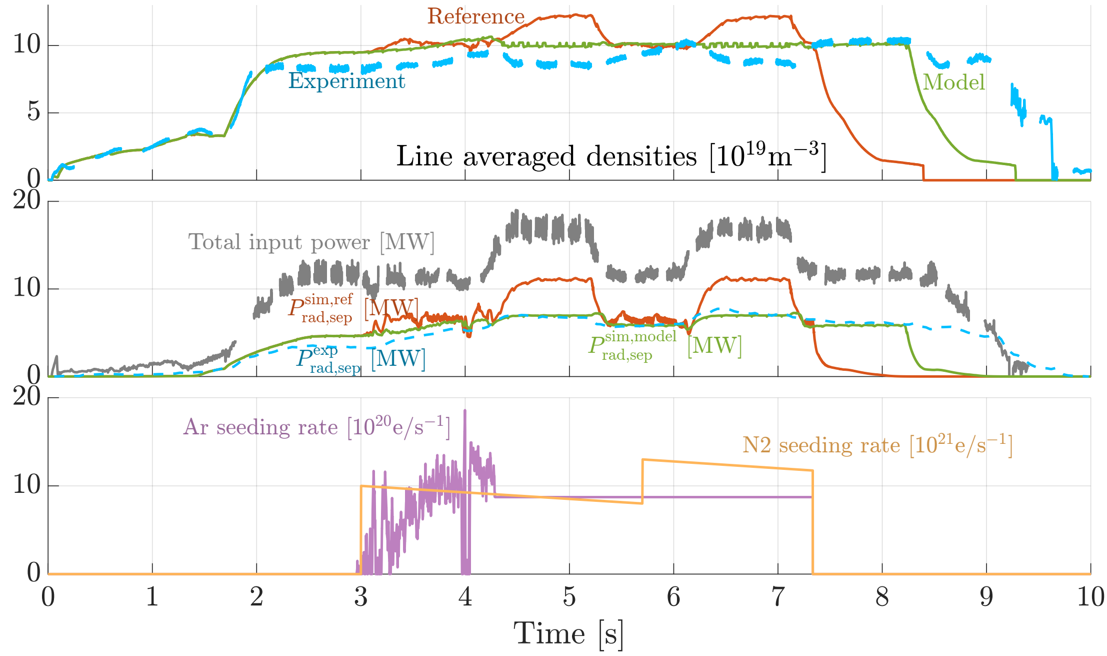

Figure 4: Density (top), power balance (middle) and impurities seeding rates (bottom) for discharge 40250 and its Fenix simulation. The simulation traces are shown without (red – 'ref' or 'reference') and with (green – 'model') the impurity model. The seeding rate are the same for both the experiment and simulations.

inputs. In both subplots, the light blue trace is the experimental case, and in red and green are simulations without and with the impurity model from [KDH+24], respectively. The total input power is also shown in dark blue. Using the impurity model, the radiated power does not directly follow the changes in heating power during the two NBI steps at 4.2 and 6.2 s anymore, and instead stays almost constant, matching the experimental behaviour. The same behaviour is observed from the density, as the lowered radiation increases the temperature, and therefore lowers the density due to the constant pressure. No individual optimization of the density has been done, for instance by changing the transport coefficients. While the general trend is corrected, the density is still only within 11 % of the experimental values on average between 2 and 8 seconds. However, the improvement of simulations with impurities is significant enough, without resorting of the heavier model of STRAHL, to enable, for instance, the investigation of radiation controllers, as is the focus of the next subsection.

3.3 P_{sep} controller

With an updated impurity model, we can now test an upcoming controller on AUG, that will control the power crossing the separatrix P_{sep} by injecting heavy impurities (typically krypton or xenon) for core radiation. P_{sep} is the sum of all input power (NBI, ECRH and ICRH – P_{NBI}, P_{ECRH} and P_{ICRH} respectively), minus the variation of internal energy ($\frac{\mathrm{d}W}{\mathrm{d}t}$) and the radiation inside the separatrix ($P_{\mathrm{rad,sep}}$): $P_{\mathrm{sep}} = P_{\mathrm{NBI}} + P_{\mathrm{ECRH}} + P_{\mathrm{ICRH}} - \frac{\mathrm{d}W}{\mathrm{d}t} - P_{\mathrm{rad,sep}}$. To simplify the synthetic diagnostic, we will omit the $\frac{\mathrm{d}W}{\mathrm{d}t}$ term, which also results in slightly more stringent test conditions due to its negative sign, matching that of the actuator ($P_{\mathrm{rad,sep}}$). Based on the ongoing development of a diagnostic to measure $P_{\mathrm{rad,sep}}$ described in [DBP+21] adapted to real time use, a benchmark has been made to estimate the uncertainty of the real time capable version, using a set of 214 phantom images and synthetic measurements. The diagnostic has been estimated to have a 5.5 % mean error, with a 14.9 % variance. These values have been added as noise parameters to the radiated power computed in Fenix, and are used to compute the reference signal P_{sep} for the controller. The effect of the controller has

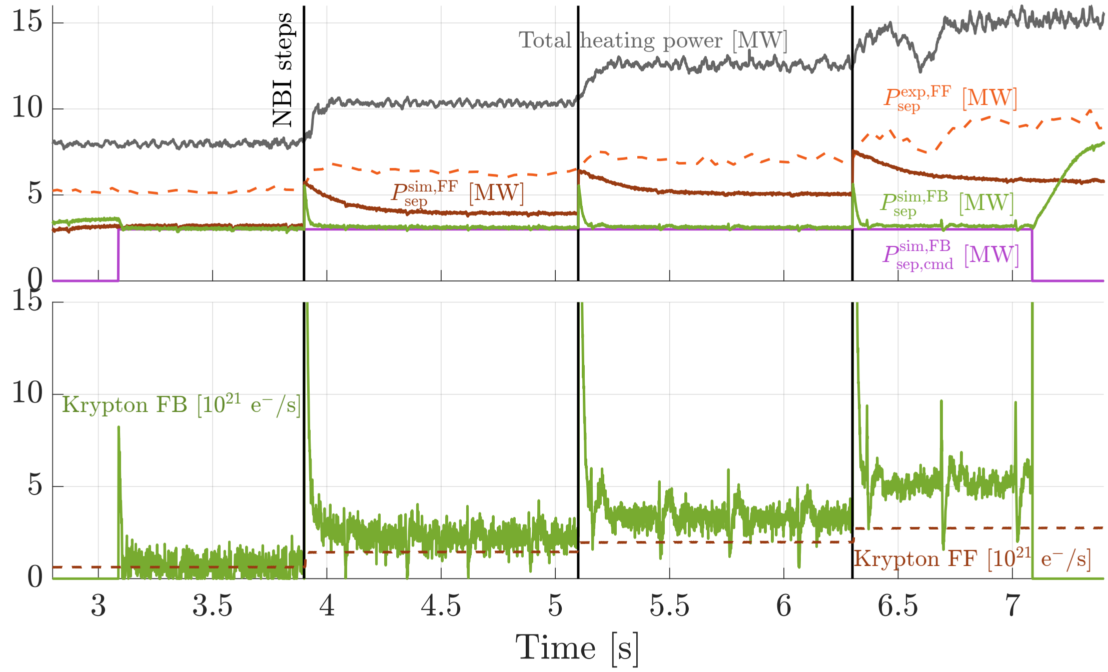

Figure 5: Total input power and P_{sep} (top) and Krypton seeding level (bottom) for discharge 39061. FF = feedforward, FB = feedback, exp = experiment, sim = simulation. Experimental traces are in lighter, dashed lines, and simulation results are in darker, solid lines. The vertical black lines shows the times of the NBI steps. The experiment is only in FF, whereas the simulation have been performed with both FF and FB.

then been tested against AUG discharge 39061, where feedforward krypton seeding steps tried to keep P_{sep} constant along three NBI steps of about 2.5 MW each. Figure 5 shows the experiment time traces, along with both a simulation of the same feedforward inputs and one using the feedback P_{sep} controller. The red traces are from the feedforward simulation (full line, dark red) and experiment (dashed line, light red), whereas the green lines are for the simulation with feedback control enabled, for which the purple line shows the P_{sep} reference signal. The green traces show that the target constant value of 3 MW can be followed within 0.2 MW after a convergence time bellow 100 ms for each power step. The convergence time depends on the exact characteristic times of the power step and of krypton transport from the gas valve to the confined plasma compared. While the convergence time depends on the controller gains, fine tuning them in Fenix would first require a fine calibration of the krypton transport time, currently largely overestimated. However, if that is done, Fenix could also be used for system identification of the P_{sep} controller without using experimental time. It is foreseen to implement and test the controller in the upcoming AUG campaign, and the tests using Fenix allowed to validate the scenario and plasma stability despite the delay of the gas valves.

3.4 Plasma vertical (in)stability (#39655)

This subsection presents a simulation of discharge #39655, where the controllers for plasma vertical position and plasma shape have been frozen at 2.99 s, *i.e.* the voltage of all control coils is then fixed at their last value. A so called vertical displacement event (VDE) shortly followed, where the plasma disrupts by vertical instability, due to its elongation. The goal of the simulation is to showcase the dynamic of the loop for magnetic control of Fenix, including the newly developed equilibrium solver [FTGt25]. Figure 6 shows time traces of the discharge for both the experiment and simulation, between shortly before freezing the magnetic controllers and the plasma disruption. The density and plasma current traces allow to follow the time of disruption. The plasma vertical position, depicted by vertical position of the center of the plasma current

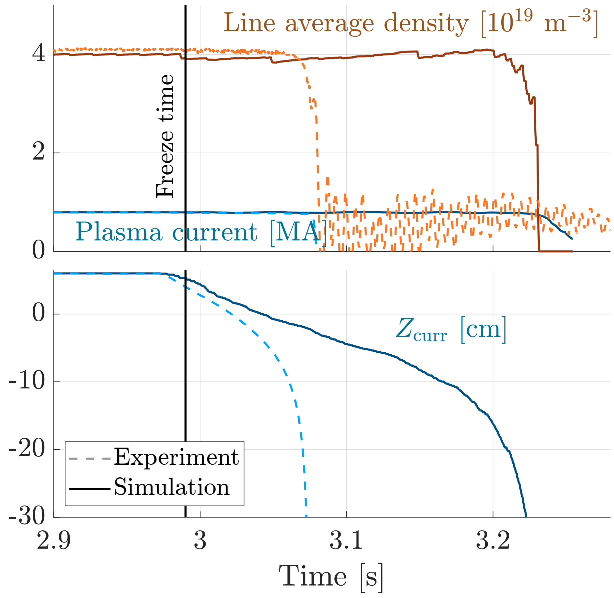

Figure 6: Plasma current and density (top) and vertical position $Z_{\rm curr}$ (bottom) for discharge 39655 and its Fenix simulation. Experimental traces are in lighter, dashed lines, and simulation results are in darker, solid lines. The vertical black line shows the time when the controllers were frozen.

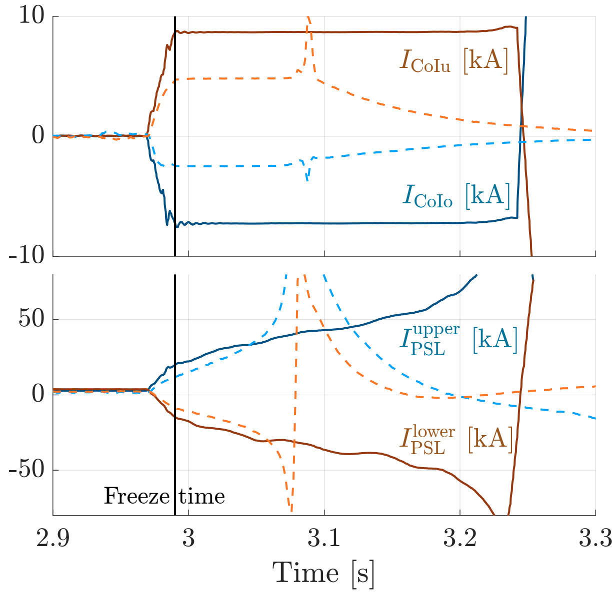

Figure 7: Currents in the in-vessel position control coils 'CoI' (top) and the in-vessel passive stabilizing loops 'PSL' (bottom), of the upper (blue) and lower (orange) part of the vessel for discharge 39655 (dashed and lighter) and its Fenix simulation (solid and darker). The black line shows when the controllers were frozen.

$Z_{\rm curr}$, shows a slower drift in the simulation. Figure 7 displays the evolution of the in-vessel coil currents. The time evolution from simulation displays a similar general behaviour as in the experiment. The plasma starts becoming unstable 20 ms before the freezing time. In the simulations, the in-vessel coils used for the plasma vertical stabilization CoIo (upper part of the vessel) and CoIu (lower part of the vessel) evolve faster, despite a lower plasma vertical displacement and slightly larger current induced in the in-vessel passive stabilizer loop (PSL), and therefore end up freezing at larger (respectively positive and negative) currents. The later disruption in Fenix is partly due to the slower vertical displacement of the plasma. It has been checked that it can be corrected by either decreasing the ASTRA time step or by running the full non-linear Grad-Shafranov solver iterations, allowing faster movement of the plasma by ensuring that the solver can fully converge at each time step. The time at which the current quench triggers can also be adjusted by adjusting the transport coefficients. However, as already mentioned, it is chosen to only showcase the generic capabilities of Fenix, without fine tuning for each purpose, which is usually the topic of dedicated work. In the current case, the simulation fits the experiment up to the thermal quench, at which point the implemented model becomes deficient, as MHD related transport mechanisms and current quench models are not included.

3.5 Upper divertor test

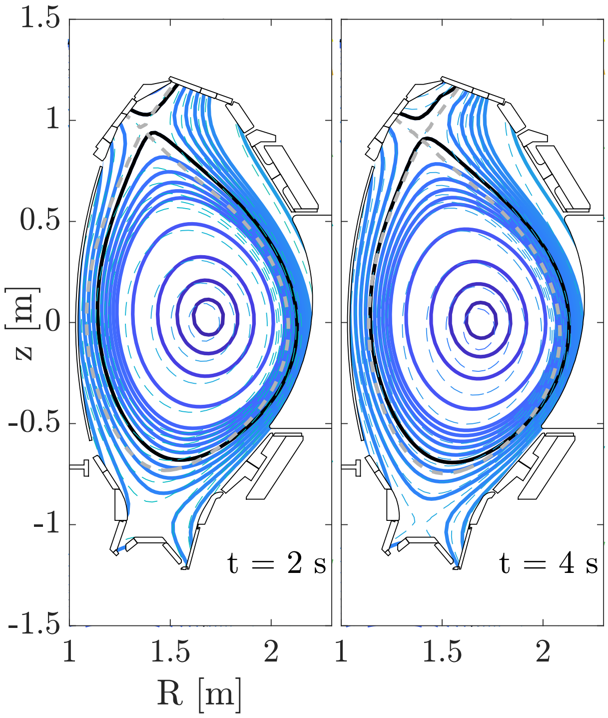

Figure 8: Magnetic contour of the plasma in the simulation of #36284 without the upper divertor coils. The experimental contours are shown in thinner, dashed lines. The vessel wall is the one for the last campaigns before 2023.

The last example shown here is about the use of the coils in the new upper divertor of AUG [HTZ+17, ZHW+24]. These two coils, called Doa and Doi, allow for new divertor leg and X-point configurations when doing upper single null discharges. Using the position and size of the new coils, as well as their foreseen power supply configurations, it is possible to run Fenix simulations and look at the effect of new coils on a discharge. To do so we will use the reference AUG discharge #36284 that had an upper single null shape, as shown in Figure 8. The reference simulation shows a magnetic equilibrium (full lines) that slightly differs from the reconstructions of the experiment (dashed lines), mostly due to different kinetic profiles. In the future, the computation of the magnetic equilibrium will also benefit from better optimized transport and source parameters. Once adding the upper divertor coils and their requested currents for Doa and Doi, the simulation shows a change of the outer divertor leg shape, as can be seen at 4 s (right plot), compared to the time without Doa and Doi $t = 2$ s (left plot, similar to the reference discharge). Furthermore, the simulation shows that the requested currents in the other shaping coils can still be followed, and their voltages are only weakly affected by the additional induced currents, as shown in Figure 9. One can see the compensating

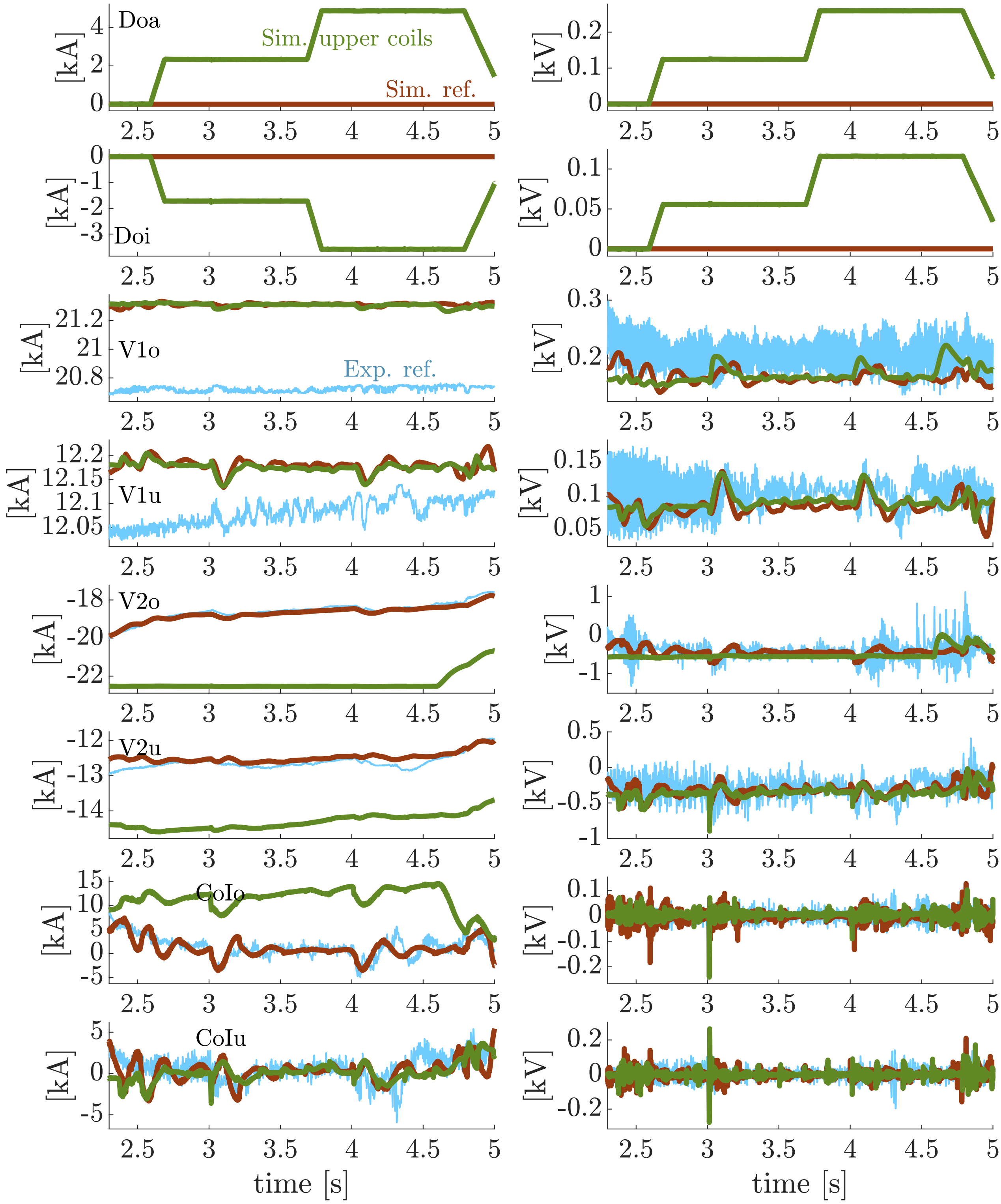

Figure 9: Coil currents for the upper single null discharge #36284 (blue) and its simulation (red), and the simulation of the same discharge with added coils of the new AUG upper divertor (green).

command voltages when the current in Doa and Doi are increased, before going back to their original values.

The most affected coils are the other in-vessel coils CoIu and CoIo, used to vertically stabilize the plasma. Nonetheless, they are still way below their operational limits of 25 kA, and the plasma is kept in place during the two current ramps. The resulting forces and energy consumption can also be estimated, and will be compared to the foreseen machine limits for new scenarios, in order to assist the next experimental campaign of AUG. So far, these preliminary simulations validate the expected behaviour of the upper divertor. Once the first experimental measurements will be available, their comparison with the expectations from the simulation will further help advancing in the planning and trust of future discharges.

4 Conclusion

The newest version of Fenix AUG proved to have a good versatility, and, despite its limitations, its default configuration is reliable enough to assess, for instance, new physics models, controllers or scenarios. The code management and the configuration to given AUG setups have now been made robust, and follow basic coding standards. Furthermore, many independent advancements have been made to the structure of Fenix AUG and many of its models, only the main ones being reported in table 1. Ultimately, despite the high complexity of the flight simulator, the combination of all the mentioned changes and the significant improvements to the user-friendliness opens the usability by non specialized users.

The ability to run headless simulations will become the next focus. With the capacity to run Fenix AUG in batches, better opportunities to optimize the model's free parameters will arise, and the quantification of results and benchmarks will gain significantly more relevance. The numerous use cases also revealed limitations and therefore initiated upcoming upgrades for the models, especially for the power plant. Notably, the power consumption is mostly over-estimated in Fenix compared to the experiment and needs to be improved. In general, the different models within Fenix are being updated to try to follow the state of the art.

Finally, since Fenix is used for AUG, DEMO, ITER and TCV, updates to the structure or the models can come from any of the implementation and influence the others, which is an added strength for comparison and collaboration.

Acknowledgments

This work has been carried out within the framework of the EUROfusion Consortium, funded by the European Union via the Euratom Research and Training Programme (Grant Agreement No 101052200 — EUROfusion). Views and opinions expressed are however those of the author(s) only and do not necessarily reflect those of the European Union or the European Commission. Neither the European Union nor the European Commission can be held responsible for them.

References

[AGT+22] C. Angioni, T. Gamot, G. Tardini, E. Fable, T. Luda, N. Bonanomi, C. Kiefer, G. Staebler, the ASDEX Upgrade Team, and the EUROfusion MST1 Team, Confinement properties of L-mode plasmas in ASDEX Upgrade and full-radius predictions of the TGLF transport model, *Nuclear Fusion* **62** no. 6 (2022), 066015. doi:10.1088/1741-4326/ac592b.

[BvG+23] H.-S. Bosch, P. van Eeten, O. Grulke, T. Bräuer, S. Degenkolbe, M. Nagel, T. Rummel, J. Schacht, A. Spring, and A. Winter, Preparing the operation of Wendelstein 7-X in the steady-state regime, *Fusion Engineering and Design* **193** (2023), 113830. doi:10.1016/j.fusengdes.2023.113830.

[CFS+24] C. Coosemans, E. Fable, O. Sauter, P. David, F. Felici, C. Galperti, A. Mele, A.Merle, A. Tenaglia, C. Wu, and the TCV Team, *Application of the Fenix flight simulator to TCV*, Poster at the 50st EPS conference on Controlled Fusion and Plasma Physics 8-12 July 2024, (2024). Available at https://lac913.epfl.ch/epsppd3/2024/html/PDF/P4-102.pdf.

[DBP+21] P. David, M. Bernert, T. Pütterich, C. Fuchs, S. Glöggler, T. Eich, and the ASDEX Upgrade Team, Optimization of the computation of total and local radiated power at ASDEX Upgrade, *Nuclear Fusion* **61** no. 6 (2021), 066025. doi:10.1088/1741-4326/abf2e1.

[dCD+24] P. de Vries, M. Cinque, G. De Tommasi, W. Treutterer, D. Humphreys, M. Walker, F. Felici, I. Gomez, L. Zabeo, T. Ravensbergen, and others, Strategy to systematically design and deploy the ITER plasma control system: A system engineering and model-based design approach, *Fusion Engineering and Design* **204** (2024), 114464. doi:10.1016/j.fusengdes.2024.114464.

[dFF+23] L. E. di Grazia, E. Fable, D. Frattolillo, M. Mattei, P. David, and C. Wu, Development of magnetic control for the EU-DEMO flight simulator and application to transient phenomena, *Fusion Engineering and Design* **191** (2023), 113579. doi:10.1016/j.fusengdes.2023.113579.

[Dux06] R. Dux, *STRAHL User Manual*, Tech. Rep. 10/30 IPP Garching Garmany, (2006).

[FJT+22] E. Fable, F. Janky, W. Treutterer, M. Englberger, R. Schramm, M. Muraca, C. Angioni, O. Kudlacek, E. Poli, M. Reich, and others, The modeling of a tokamak plasma discharge, from first principles to a flight simulator, *Plasma Physics and Controlled Fusion* **64** no. 4 (2022), 044002. doi:10.1088/1361-6587/ac466b.

[FTGt25] E. Fable, G. Tardini, L. Giannone, and the ASDEX Upgrade Team, FEQIS: A free-boundary equilibrium solver for integrated modeling of tokamak plasmas, *Open Plasma Science* **1** no. 2 (2025). doi:10.46298/ops.14641.

[FAD+24] D. Fajardo, C. Angioni, R. Dux, E. Fable, U. Plank, O. Samoylov, G. Tardini, and the ASDEX Upgrade Team, Full-radius integrated modelling of ASDEX Upgrade L-modes including impurity transport and radiation, *Nuclear Fusion* **64** no. 4 (2024), 046021. doi:10.1088/1741-4326/ad29bd.

[HTZ+17] A. Herrmann, M. Teschke, I. Zammuto, M. Faitsch, A. Kallenbach, K. Lackner, T. Lunt, R. Neu, M. Rott, G. Schall, and others, An optimized upper divertor with divertor-coils to study enhanced divertor configurations in ASDEX Upgrade, *Fusion Engineering and Design* **123** (2017), 508–512, Proceedings of the 29th Symposium on Fusion Technology (SOFT-29) Prague, Czech Republic, September 5-9, 2016. doi:10.1016/j.fusengdes.2017.05.074.

[JFET21] F. Janky, E. Fable, M. Englberger, and W. Treutterer, Validation of the Fenix ASDEX Upgrade flight simulator, *Fusion Engineering and Design* **163** (2021), 112126. doi:10.1016/j.fusengdes.2020.112126.

[KDH+24] A. Kallenbach, R. Dux, S. Henderson, C. Tantos, M. Bernert, C. Day, R. McDermott, V. Rohde, A. Zito, and the ASDEX Upgrade Team, Divertor enrichment of recycling impurity species (He, N2, Ne, Ar, Kr) in ASDEX Upgrade H-modes, *Nuclear Fusion* **64** no. 5 (2024), 056003. doi:10.1088/1741-4326/ad3139.

[KDG+24] O. Kudláček, P. David, I. Gomez, A. Gräter, B. Sieglin, W. Treutterer, M. Weiland, T. Zehetbauer, M. V. Berkel, M. Bernert, and others, Overview of advances in ASDEX Upgrade plasma control to support critical physics research for ITER and beyond, *Nuclear Fusion* **64** no. 5 (2024), 056012. doi:10.1088/1741-4326/ad3472.

[KTS+20] O. Kudláček, W. Treutterer, B. Sieglin, F. Janky, F. Felici, I. Gomez-Ortiz, A. Gräter, T. Maceina, M. Maraschek, and T. Zehetbauer, Use of virtual actuators in ASDEX Upgrade control, *Fusion Engineering and Design* **159** (2020), 111735. doi:10.1016/j.fusengdes.2020.111735.

[KcB+21] G. M. Kurtzer, cclerget, M. Bauer, I. Kaneshiro, D. Trudgian, and D. Godlove, hpcng/singularity: Singularity 3.7.3, (2021). doi:10.5281/zenodo.4667718.

[KGS+15] C.-P. Käsemann, E. Grois, F. Stobbe, M. Rott, and K. Klaster, Pulsed power supply system of the ASDEX upgrade Tokamak research facility, in *2015 IEEE 15th International Conference on Environment and Electrical Engineering (EEEIC)*, (2015), pp. 237–242. doi:10.1109/EEEIC.2015.7165545.

[LAD+20] T. Luda, C. Angioni, M. Dunne, E. Fable, A. Kallenbach, N. Bonanomi, P. Schneider, M. Siccinio, G. Tardini, the ASDEX Upgrade Team, and the EUROfusion MST1 Team, Integrated modeling of ASDEX Upgrade plasmas combining core, pedestal and scrape-off layer physics, *Nuclear Fusion* **60** no. 3 (2020), 036023. doi:10.1088/1741-4326/ab6c77.

[MTtI08] Y. R. Martin, T. Takizuka, and the ITPA CDBM H-mode Threshold Data Group, Power requirement for accessing the H-mode in ITER, *Journal of Physics: Conference Series* **123** (2008), 012033. doi:10.1088/1742-6596/123/1/012033.

[Mat22] MathWorks Inc., MATLAB version: 9.13.0 (R2022b), (2022). Available at https://www.mathworks.com.

[Mer14] D. Merkel, Docker: lightweight Linux containers for consistent development and deployment, *Linux journal* **2014** no. 239 (2014), 2. Available at https://dl.acm.org/doi/10.5555/2600239.2600241.

[MP19] K. Meyer and J. Padayachee, Advancements in plasma control supervision, *Journal of Fusion Energy* **38** (2019), 437–444. doi:10.1007/s10894-018-0190-1.

[NER+07] G. Neu, K. Engelhardt, G. Raupp, W. Treutterer, D. Zasche, and T. Zehetbauer, The ASDEX Upgrade discharge schedule, *Fusion Engineering and Design* **82** no. 5 (2007), 1111–1116, Proceedings of the 24th Symposium on Fusion Technology. doi:10.1016/j.fusengdes.2006.12.003.

[NMS+23] R. Nouailletas, P. Moreau, B. Santraine, J. Colnel, C. Reux, Y. Moudden, S. Darche, and N. Amiot, WEST plasma control system status, *Fusion Engineering and Design* **192** (2023), 113582. doi:10.1016/j.fusengdes.2023.113582.

[SNL+06] J. Schacht, H. Niedermeyer, H. Laqua, A. Spring, I. Müller, S. Pingel, and A. Wölk, Tasks and structure of the WENDELSTEIN 7-X control system, *Fusion Engineering and Design* **81** no. 15 (2006), 1799–1806, 5th IAEA TM on Control, Data Acquisition, and Remote Participation for Fusion Research. doi:10.1016/j.fusengdes.2006.04.045.

[TFA+24] G. Tardini, E. Fable, C. Angioni, D. Fajardo, and the ASDEX Upgrade Team, *ASTRA modularity and IMASification for integrated modelling workflows*, Poster at the 27th Joint EU-US Transport Task Force Meeting 11-15 Sep 2023, (2024). Available at https://ttf2023.sciencesconf.org/data/pages/Bookletwcover.pdf.

[TCL+14] W. Treutterer, R. Cole, K. Lüddecke, G. Neu, C. Rapson, G. Raupp, D. Zasche, and T. Zehetbauer, ASDEX upgrade discharge control system—a real-time plasma control framework, *Fusion Engineering and Design* **89** no. 3 (2014), 146–154, Design and implementation of real-time systems for magnetic confined fusion devices. doi:10.1016/j.fusengdes.2014.01.001.

[TRR+17] W. Treutterer, C. Rapson, G. Raupp, J. Snipes, P. de Vries, A. Winter, D. Humphreys, M. Walker, G. de Tommasi, M. Cinque, and others, Towards a preliminary design of the ITER plasma control system architecture, *Fusion Engineering and Design* **115** (2017), 33–38. doi:10.1016/j.fusengdes.2016.12.026.

[TZM+05] W. Treutterer, T. Zehetbauer, V. Mertens, G. Neu, G. Raupp, and D. Zasche, Plasma feedback controller reorganisation for ASDEX Upgrade's new discharge control and data acquisition system, *Fusion Engineering and Design* **74** no. 1 (2005), 501–505, Proceedings of the 23rd Symposium of Fusion Technology. doi:10.1016/j.fusengdes.2005.06.151.

[WAD+15] M. Walker, G. Ambrosino, G. De Tommasi, D. Humphreys, M. Mattei, G. Neu, C. Rapson, G. Raupp, W. Treutterer, A. Welander, and A. Winter, The ITER plasma control system simulation platform, *Fusion Engineering and Design* **96-97** (2015), 716–719, Proceedings of the 28th Symposium On Fusion Technology (SOFT-28). doi:10.1016/j.fusengdes.2015.01.009.

[WDF+24] C. Wu, P. David, E. Fable, D. Frattolillo, L. E. Di Grazia, M. Mattei, M. Siccinio, W. Treutterer, and H. Zohm, Architecture design and internal implementation of a universal coupling between controllers and physics in a tokamak flight simulator, *Fusion Science and Technology* **80** no. 6 (2024), 766–771. doi:10.1080/15361055.2023.2234741.

[WSW+21] H. Wu, F. Subba, M. Wischmeier, M. Cavedon, R. Zanino, and the ASDEX Upgrade Team, SOLPS-ITER modeling of ASDEX Upgrade L-mode detachment states, *Plasma Physics and Controlled Fusion* **63** no. 10 (2021), 105005. doi:10.1088/1361-6587/ac1568.

[YGY+21] Q. Yuan, H. Guo, L. Yan, Z. Huang, J. Huang, B. Xiao, Y. Zheng, R. Zhang, and Z. Luo, Preliminary design of real-time plasma control system for CFETR, *Fusion Engineering and Design* **173** (2021), 112876. doi:10.1016/j.fusengdes.2021.112876.

[ZHW+24] I. Zammuto, A. Herrmann, M. Weissgerber, V. Brack, V. Rohde, G. Schall, M. Teschke, T. Vierle, S. Vorbrugg, B. Petzold, and others, Status of the project: New upper divertor with coils in ASDEX Upgrade, *IEEE Transactions on Applied Superconductivity* **34** no. 5 (2024), 1–6. doi:10.1109/TASC.2023.3344543.